ICAS Paper No. 68-14

EXPERIMENTAL VERIFICATION OF SHOCK FREE TRANSONIC FLOW AROUND QUASI-ELLIPTICAL AEROFOIL SECTIONS

by

B. M. Spee and R. Uijlenhoet
Aerodynamics Division
National Aerospace Laboratory
Amsterdam, Netherlands

The Sixth Congress of the International Council of the Aeronautical Sciences

DEUTSCHES MUSEUM, MÜNCHEN, GERMANY/SEPTEMBER 9-13, 1968

Preis: DM 2.00

EXPERIMENTAL VERIFICATION OF SHOCK-FREE TRANSONIC FLOW AROUND QUASI-ELLIPTICAL AEROFOIL SECTIONS

B.M. Spee and R. Uijlenhoet

National Aerospace Laboratory NLR, Amsterdam

Summary

Wind tunnel experiments have been performed on a series of symmetrical quasi-elliptical aerofoil sections, designed for zero lift and exhibiting different types of supercritical pressure distributions.

The experimental data are in close agreement with the theoretical results and demonstrate the physical relevance of theoretical potential flows. At least in a practical sense, shock-free flow has been obtained for all aerofoils. The results suggest that the discrepancies between experiment and theory can be made arbitrarily small by eliminating model imperfections and boundary layer effects.

The shock-free design condition is embedded in an interval of free stream Mach numbers and incidences where the wave drag appears to be negligible.

Introduction

The possibility of isentropic recompression from supersonic to subsonic speeds in two-dimensional transonic flows, a controversial subject in the past, has first been demonstrated by Pearcey. He developed, on an experimental basis, profile flows which are in a practical sense shock free.

The advent of Nieuwland's theory of quasi-elliptical aerofoils (ref.1 and 2) offers, for the first time, the opportunity for a systematical experimental investigation of profile shapes defined by mathematical transonic potential flow solutions.

Although now several examples of theoretical solutions for the transonic potential flow around lifting quasi-elliptical aerofoils are available, the wind tunnel experiments described in this paper have been performed on symmetrical aerofoils, that is on aerofoils designed for zero lift. The reason for this is that the latter were much earlier available. This means, of course, that in a practical sense the value of the investigation is rather limited. However, the fundamental problems of two-dimensional shock free transonic flow can quite satisfactorily be studied in the symmetrical case.

From an experimental point of view, the relatively simple symmetric flow has important benefits. The absence of large wall interference and boundary layer effects on circulation makes the interpretation of the results easier and more reliable

List of symbols

c	chord length
c_d	drag coefficient, $D/q.c.$
D	drag
M	free-stream Mach number
p	static pressure
p_o	stagnation pressure
q	dynamic pressure
x	co-ordinate in chord direction
z	co-ordinate normal to the chord
α	incidence
τ, ϵ, λ	aerofoil parameters
$( )^*$	sonic value
$( )_t$	wind tunnel conditions

Aerofoils

The transonic flow around symmetrical quasi-elliptical aerofoil sections is obtained, by way of a transformation in the hodograph plane, from the incompressible flow around a non-lifting elliptical cylinder. The shape of the section and its pressure distribution can not be specified in advance, but depends upon an arbitrary large number of parameters. The section and the flow field can be determined only by explicit computation for specified values of the parameters.

A series of symmetrical quasi-elliptical aerofoils has been computed. Three parameters, τ, ϵ and λ were selected, where τ determines the free-stream Mach number and ϵ the thickness ratio. λ controls the leading-edge curvature and the rate of expansion over the forward part of the section. The parameter values have been combined such as to give different types of aerofoils and pressure distributions.

The results of the computations are given in ref.3. Having chosen the value of ϵ, the values of τ and λ are restricted to a certain region. When τ or λ, or both are chosen too large, limit lines destroy the regularity of the section and of the potential flow around it. On the other hand if λ is too small, the leading edge is cusped which makes the aerofoil less interesting from a practical and experimental point of view. All aerofoils have a cusped trailing edge. An illustration showing the τ and λ limits for a fixed value of ϵ is given in fig.1.

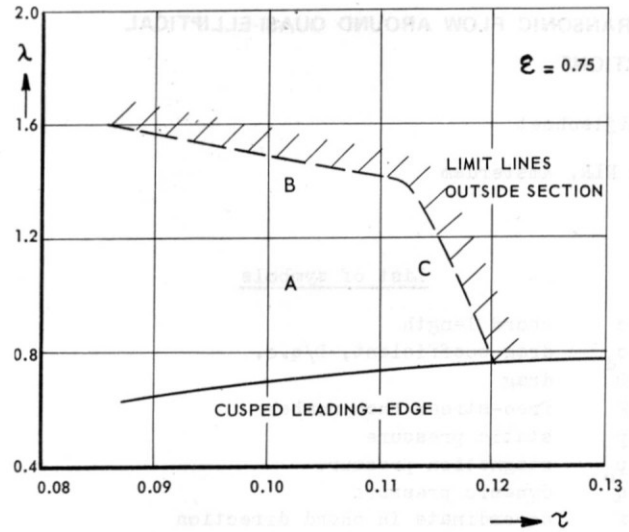

Figure 1 Admissable values of the aerofoil parameters (ε = 0.75).

The results of ref.3 show that there are three main types of pressure distributions for these symmetrical aerofoils. For moderate values of τ and λ the pressure distribution is of a smooth rooftop type (region A). When the combination of τ and λ is close to the limit, the pressure distribution is of the peaky type with a rapid expansion along the surface from the leading edge, whether or not with a secondary expansion just before the suction peak (B and C). These different types are indicated in fig.1.

From the series of aerofoils presented in ref.3, four have been chosen for the experimental investigation :

aerofoil 1 : τ = 0.11 ; ε = 0.75 ; λ = 1.375
aerofoil 2 : τ = 0.115 ; ε = 0.75 ; λ = 1.2
aerofoil 3 : τ = 0.12 ; ε = 0.8 ; λ = 1.15
aerofoil 4 : τ = 0.1 ; ε = 0.675 ; λ = 1.6

The shape of the aerofoils, the sonic lines and the pressure distributions are given in fig.2.

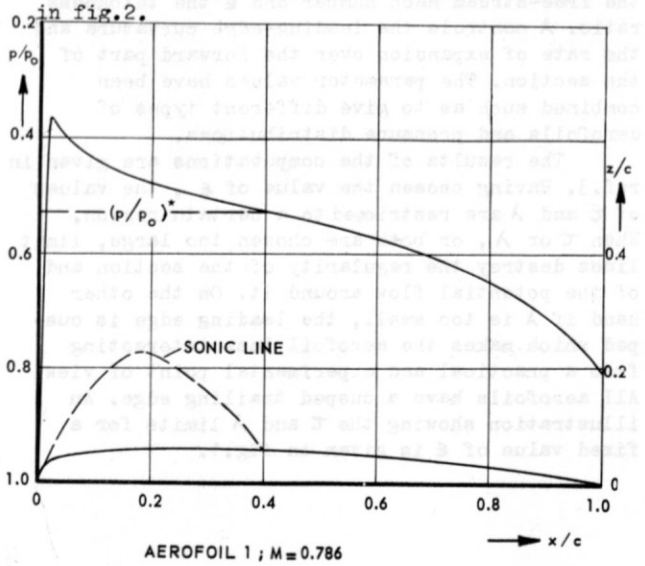

Figure 2 Aerofoil shapes, sonic lines and pressure distributions.

The pressure distributions on these aerofoils are representative for the different types that have been found in ref.3. The aerofoils 1 and 4, 12 % and 16 % thick, both have a peaky pressure distribution and a relatively small (low) supersonic region. The maximum local Mach number for aerofoil 4 (Mmax = 1.47) however is appreciably higher than for aerofoil 1 (Mmax = 1.30). Aerofoil 2, 11 % thick, exhibits a peaky distribution with a secondary expansion, aerofoil 3, 9 % thick, has a smooth pressure distribution. Aerofoils 2 and 3 both have a relatively large supersonic region.

Test details

The experiments have been performed in the transonic test section of the NLR pilot-tunnel. The test section has closed side walls and slotted top and bottom walls with an open ratio of 10 %. The stagnation pressure was about 1 atmosphere, the stagnation temperature 40° C. A detailed description of the wind tunnel is given in ref.4.

The nominal chord length of the two-dimensional models was 180 mm. The models spanned the test section (420 mm) and were supported in glass windows in the tunnel side walls. The cusped trailing edge of the aerofoils had to be partly cut off for manufacturing reasons, so that the trailing edge of the models was about 0.05 mm thick and the chord length somewhat smaller than the nominal value of 180 mm.

After the first series of tests, the model of aerofoil 1 has been corrected for the displacement effect of the boundary layer. The displacement thickness has been subtracted in each point from the theoretical contour. This resulted of course not only in a thinner model, but also shortened the chord. The corrected model had a chordlength of about 170 mm.

The models have been made of stainless steel. The required accuracy was 1 x 10^{-4} times the chord length (0.018 mm) for the first 20 % of the aerofoils and 2 x 10^{-4} for the remaining part. To obtain this accuracy, the models had to be made by way of a special technique, using profiled grinding stones. The actual shape of the models has been accurately measured and compared with the theoretical shape. The results are given in fig.3.

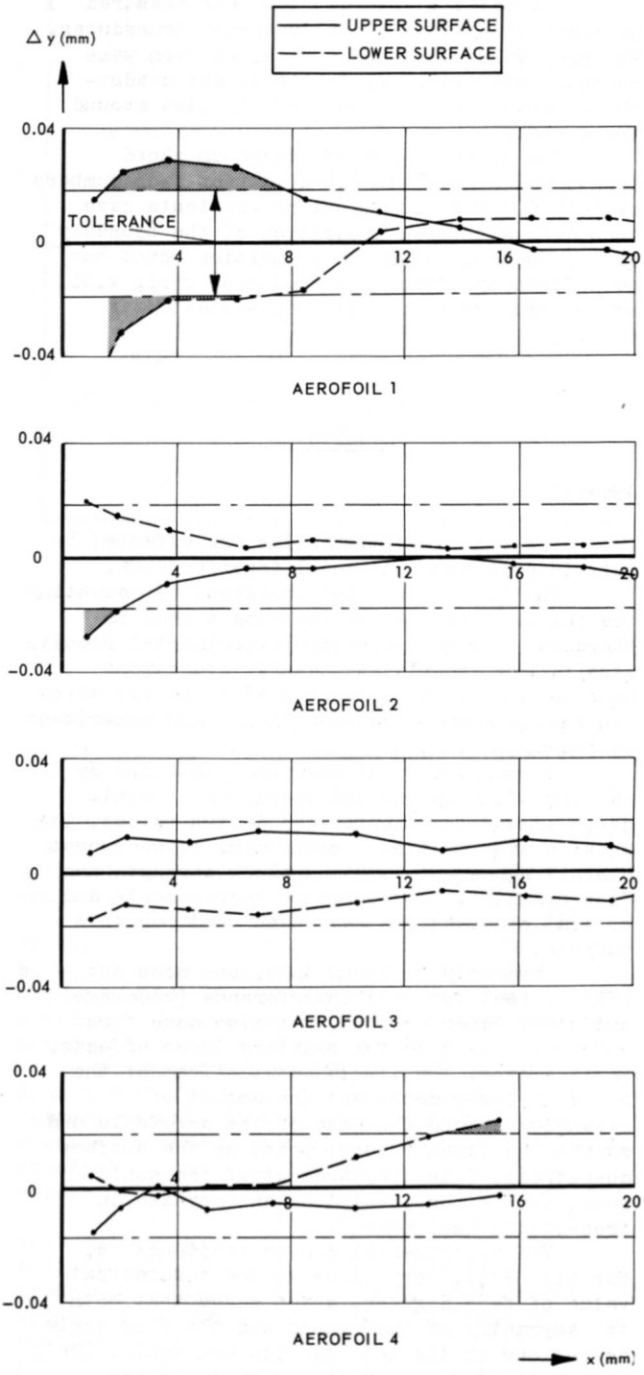

Figure 3 Accuracy of the models (nose region).

The accuracy of the models was in general, within the required values. The largest errors were found for aerofoil 1 in a region close to the leading-edge.

The models were provided with pressure holes, 0.1 mm in diameter on the front part of the aerofoils and 0.25 mm in diameter on the tail. The pressure holes were spread out over the upper and lower surface within a strip of

50 mm to avoid mutual interference of the holes.

The model pressures have been measured by means of a differential pressure transducer. The drag values have been obtained from wake pressure measurements. Schlieren and shadow-photographs have been made of the flow around the aerofoils.

The Reynolds number, based on chord length was 2 x 10^6 to 2.5 x 10^6 for Mach numbers between 0.7 and 0.85. Most of the tests have been done with free transition of the boundary layer. In some cases the transition point has been fixed by means of a roughness strip with carborundum grit to obtain consistent drag values.

Results

General

The experimental results are effected by wall interference and model imperfections.

The Mach number and incidence representing the design condition in the wind tunnel is therefore determined by the experimental results itself. The experimental design conditions have been defined as those conditions for which the best agreement between theory and experiment is found.

These conditions have been obtained by varying Mach number and incidence in small steps around the theoretical design values. The final choice is then a compromise between best overall agreement, minimum shock strength and flow symmetry. Both pressure measurements and optical observations have been used for this purpose.

Obviously by doing this, one does not only correct for wall interference (blockage) and model imperfections, but also some first correction is made for boundary layer effects. For instance, the displacement effect of the boundary layer decreases the amount of expansion around the nose of the aerofoils and shifts the forward sonic point on the surface downstream. This displacement of the sonic point can be compensated by an increase in free-stream Mach number.

The experimental design incidence is, for all cases, very close to the theoretical value of zero degrees, which means that both the asymmetry of the models and the flow angle deviations in the test section aré small. The experimental design Mach number is always higher than the theoretical value in accordance with the blockage effect in the wind tunnel which has been estimated to be -0.002 to -0.004 for these tests.

The main problem in the experiments was the appearance of laminar separation effects due to the relatively low Reynolds numbers. Oil flow tests have indicated that there are smaller or larger separation bubbles for all aerofoils, this being the main reason for the differences between experiment and theory. It is, of course, impossible to correct the models for such effects. It was shown that fixing the boundary layer transition point upstream of the separation makes the agreement between experiment and theory worse. The distortion of the model surface by the presence of a carborundum strip gives an important change in flow pattern, and leads in most cases to a pronounced shock wave.

It has already been noted that the differences between experiment and theory are very small. In fact they may be considered to be completely insignificant from a practical point of view. It should be emphasized however, that the purpose of the present tests was to get an answer on the fundamental question on the relevance of the mathematical potential flow. From that point of view, the discrepancies are significant enough to be analysed in some detail.

The design condition

The experimental and theoretical pressure distributions for aerofoils 1 and 4 are given in figs. 4 to 7.

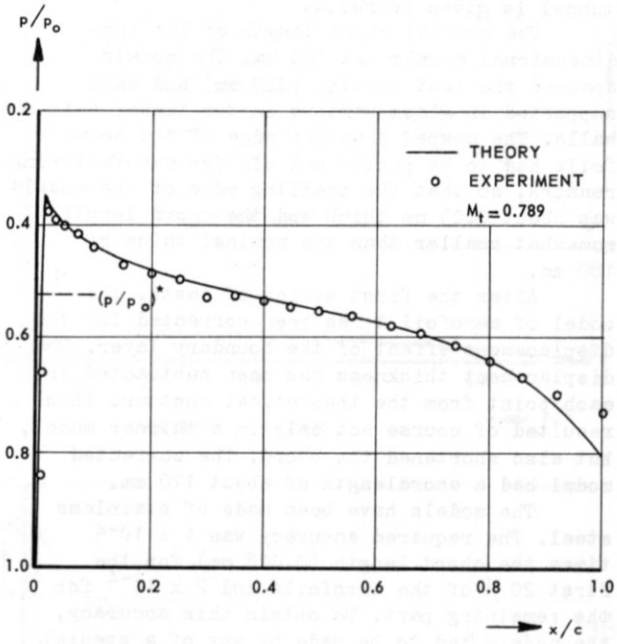

Figure 4 Experimental and theoretical pressure distribution for aerofoil 1 (x/c).

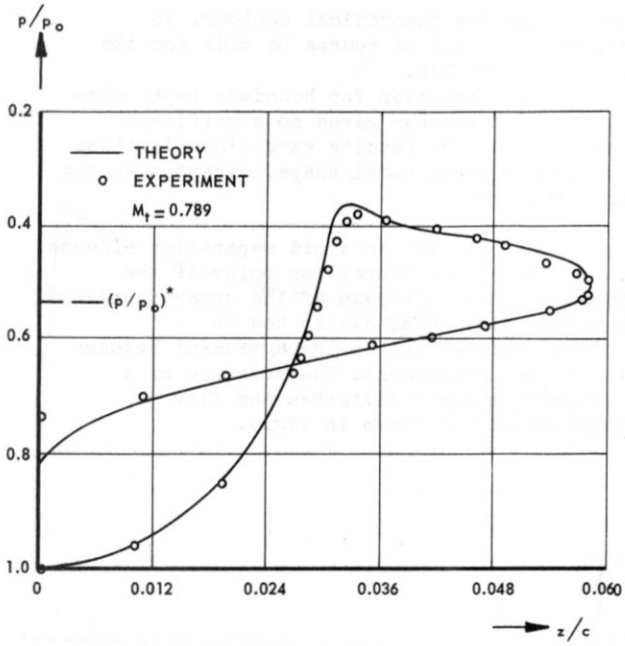

Figure 5 Experimental and theoretical pressure distribution for aerofoil 1 (z/c)

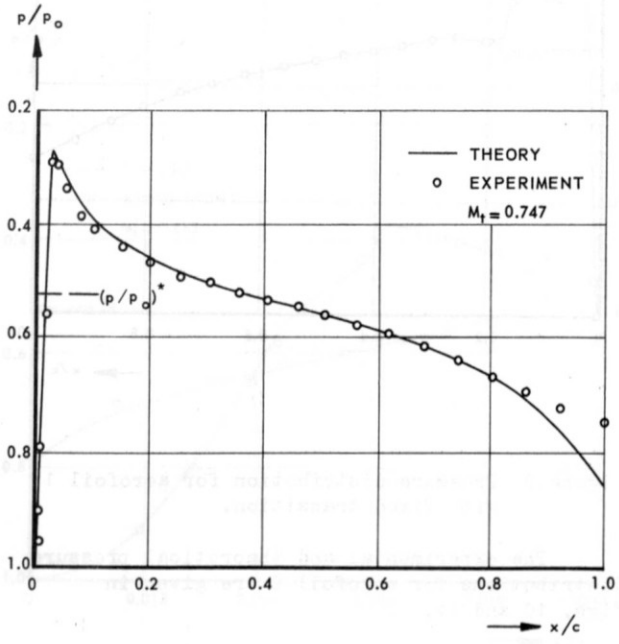

Figure 6 Experimental and theoretical pressure distribution for aerofoil 4 (x/c)

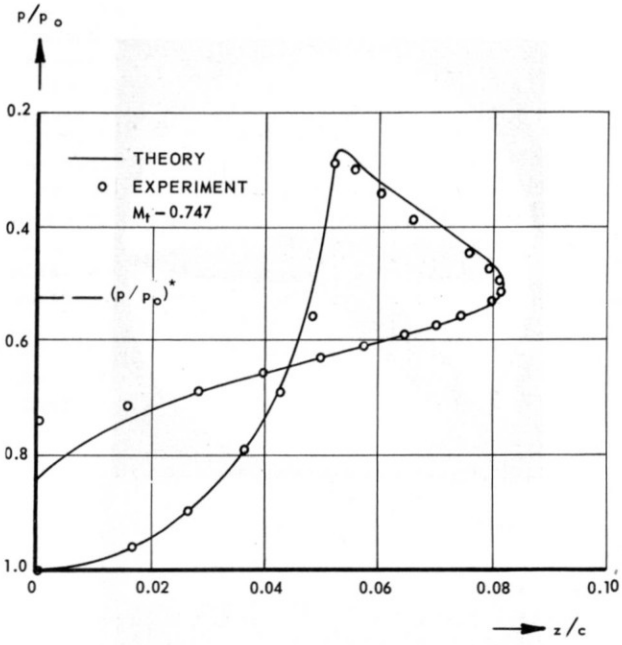

Figure 7 Experimental and theoretical pressure distribution for aerofoil 4 (z/c)

In figs. 4 and 6 the pressure is plotted against the chordwise distance measured from the leading edge, in figs. 5 and 7 against the aerofoil ordinate normal to the chord. It should be noted that the co-ordinates are based on the nominal chord length of 180 mm although the real chord length is somewhat smaller.

The experimental results shown in figs. 4 through 7 are for free transition of the boundary layer. The transition point, as obtained from acenaphtene tests was for aerofoil 1 located at 18 % of the chord and for aerofoil 4 at 12 % of the chord.

The experimental design Mach number, the Mach number for which the best agreement between experiment and theory and the weakest shock wave were obtained is, for both aerofoils, somewhat higher than the theoretical value, namely 0,003 and 0.002.

It is shown that, in general, the agreement between experiment and theory is very satisfactory. The differences between the experimental data and the theoretical curves appear to be due to model imperfections and boundary layer effects. The displacement effect of the boundary layer decreases the amount of expansion over the nose of the aerofoils as shown in figs. 5 and 7. In spite of this deficiency of expansion over the nose, the height of the suction peak is for aerofoil 4 in rather good agreement with the theoretical value. For aerofoil 1, however the suction peak is considerably too low, obviously due to local model imperfections. If such a discrepancy is interpreted as a disturbance with regard to the theoretical distribution, the influence of it will be felt downstream in the supersonic region through repeated reflections against the sonic line and the surface. Such reflections are visible on the photographs (fig.8).

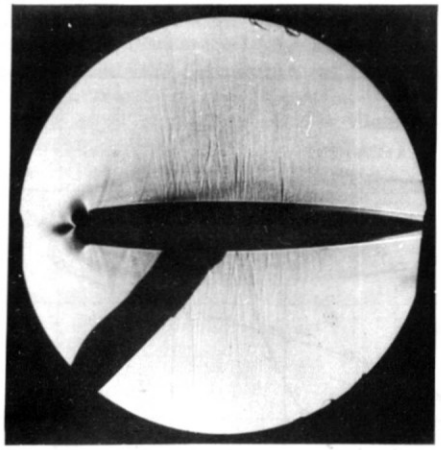

aerofoil 1; $M_t = 0.789$

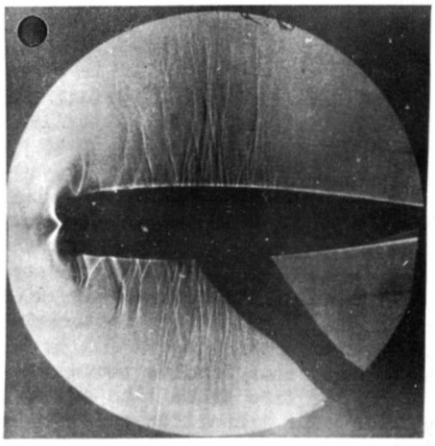

aerofoil 4; $M_t = 0.747$

Figure 8 Shadowgraphs of the flow around aerofoils 1 and 4 at the design Mach number.

It should be noted that the shadowgraphs were obtained with a short duration spark exposure that arrests upstream-moving disturbances. The disturbances form sharp pressure fronts at these speeds.

Figures 4 and 6 show that the compression behind the suction peak is larger than the theoretical compression, especially for aerofoil 4. This is due to the rapid growth of the boundary layer behind the suction peak and the presence of a small separation bubble. The difference between experiment and theory over the last 20 % of the chord is due to the rapid growth of the boundary layer close to the trailing edge.

In order to make a correction for the displacement effect of the boundary layer, the model of aerofoil 1 has been reshaped after the first series of tests. The (calculated) displacement thickness has been subtracted in each point from the theoretical contour. No correction could of course be made for the separation bubble.

The correction for boundary layer displacement thickness gives no significant improvement. The results were close to those for the original model shape, except near the trailing edge.

The only way to avoid separation effects is by fixing the transition point of the boundary layer upstream of the separation bubble. Doing this however has an unfavourable effect on the agreement between theory and experiment. The presence of a carborundum strip disturbes the flow considerably as shown in fig.9.

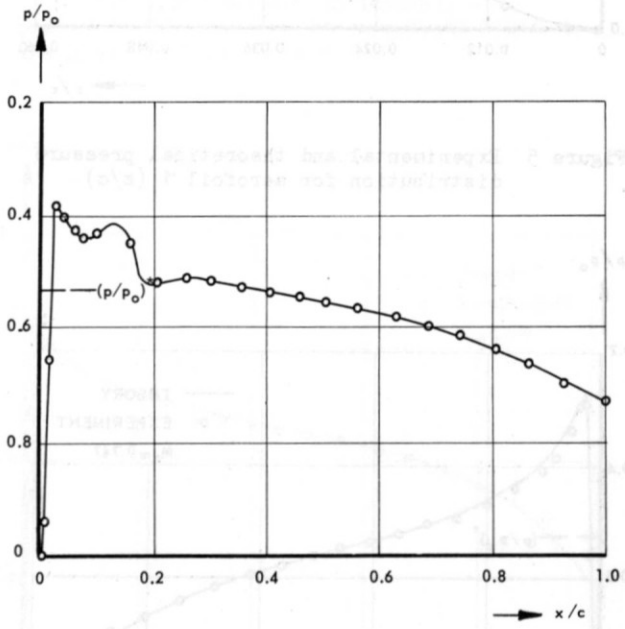

Figure 9 Pressure distribution for aerofoil 1 with fixed transition.

The experimental and theoretical pressure distributions for aerofoil 2 are given in figs. 10 and 11.

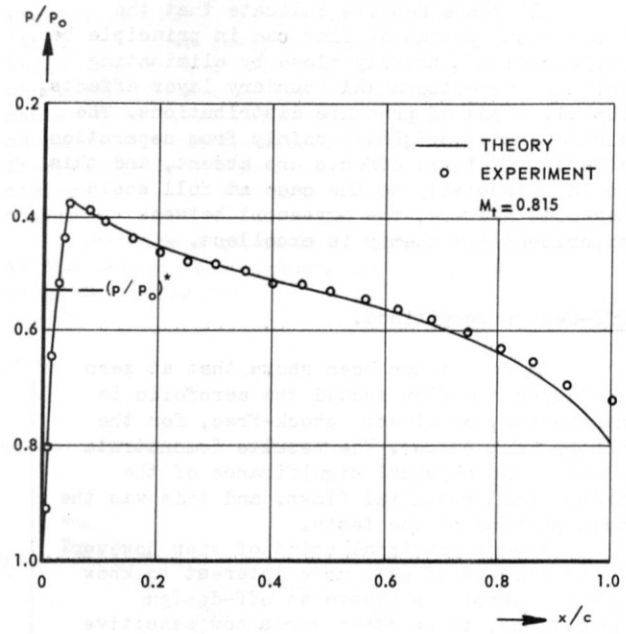

Figure 10 Pressure distribution for aerofoil 2 (x/c)

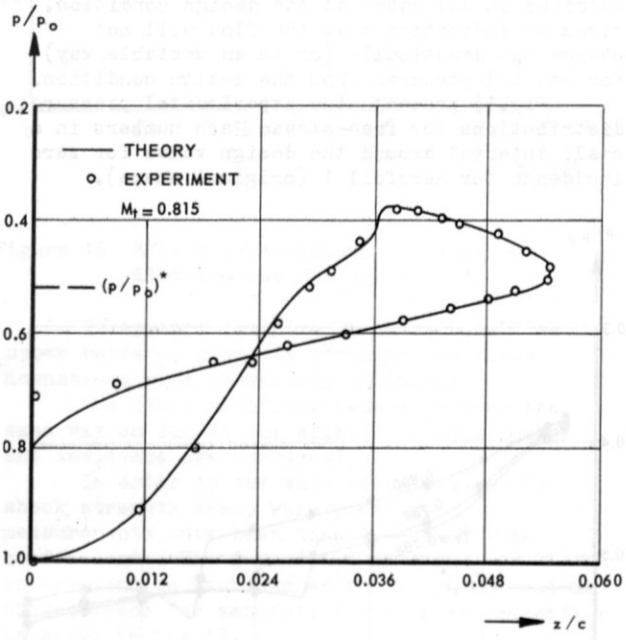

Figure 11 Pressure distribution for aerofoil 2 (z/c)

The boundary layer transition point is located at 28 % of the chord. The difference between the experimental and the theoretical design Mach number is, for this aerofoil, larger than for aerofoils 1 and 4, namely 0.009. For Mach numbers close to the theoretical design value there is a relatively large separation bubble in the laminar boundary layer. At the experimental design Mach number however this separation bubble disappears and this is the reason that in this particular case the agreement is extremely good.

Schlieren and shadowphotographs give no indication of the presence of a shock wave and the flow may be considered to be complete by shock free.

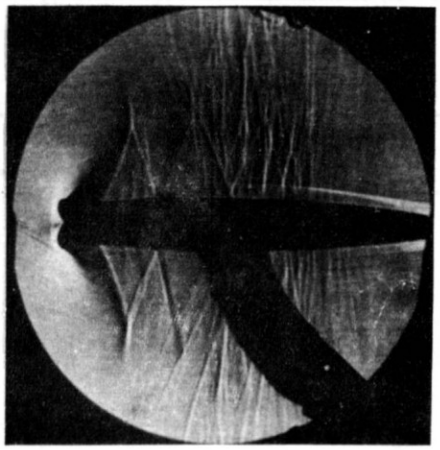

$M_t = 0.815$

Figure 12 Shadowgraph of the flow around aerofoil 2.

The pressure distribution for aerofoil 3 is given in figs. 13 and 14.

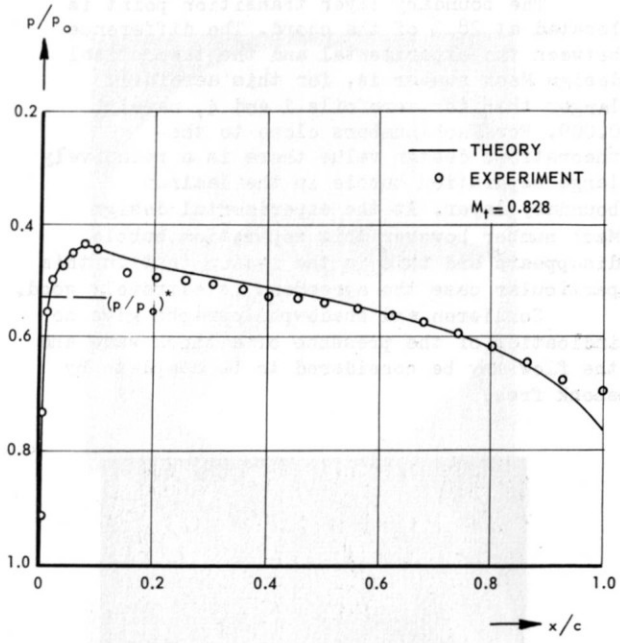

Figure 13 Pressure distribution for aerofoil 3 (x/c)

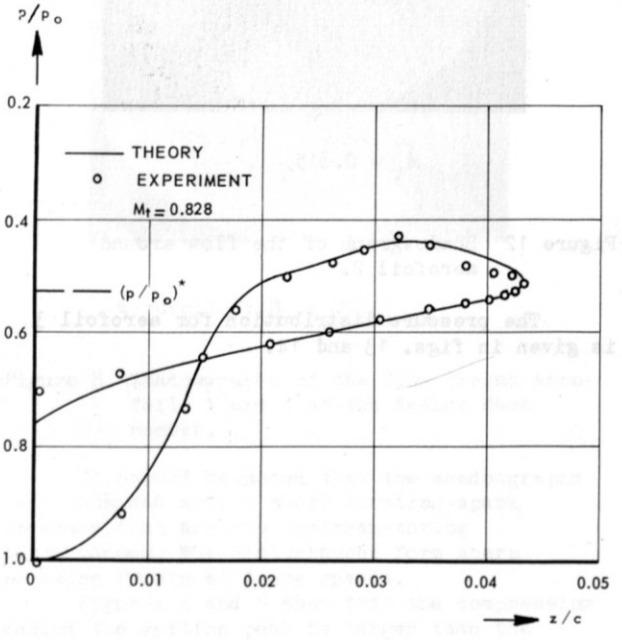

Figure 14 Pressure distribution for aerofoil 3 (z/c)

The transition point is at 25 %. For this aerofoil there is again an appreciable separation bubble in the laminar boundary layer. This separation does not disappear for higher Mach numbers and is still present at the experimental design condition. The differences between experiment and theory are larger than for the other aerofoils. In spite of this discrepancy the shock wave is weak.

All these results indicate that the theoretical potential flow can in principle be approached arbitrarily close by eliminating model imperfections and boundary layer effects, for all types of pressure distributions. The discrepancies originate mainly from separation effects. If these effects are absent, and this would undoubtedly be the case at full scale Reynolds numbers, the agreement between experiment and theory is excellent.

Off-design conditions.

So far it has been shown that at zero incidence the flow around the aerofoils is shock-free, or almost shock-free, for the design Mach number. The results demonstrate clearly the physical significance of the theoretical potential flows, and this was the main purpose of the tests.

From a practical point of view however it is perhaps of even more interest to know how the aerofoils behave at off-design conditions, or in other words how sensitive these flows are for small changes in Mach number and incidence.

The response of the flows to the presence of a transition strip indicates that in a sense they are rather sensitive. On the other hand, the fact that a stable shock-free flow has been obtained in all cases at the design condition, gives an indication that the flow will not change too drastically (or in an unstable way) for small departures from the design condition.

Fig.15 presents the experimental pressure distributions for free-stream Mach numbers in a small interval around the design value for zero incidence for aerofoil 1 (original shape).

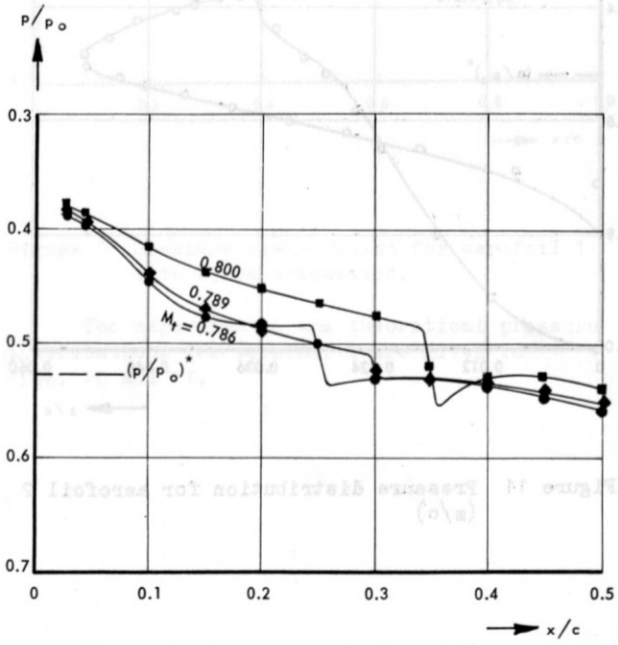

Figure 15 The effect of Mach number on pressure distribution for aerofoil 1.

These results show that the practically shock-free design condition is embedded in a family of flows involving weak shock waves both below and above the design point and that the shock-free condition can be reached in a stable manner from these neighbouring conditions. The shock wave moves downstream with increasing free-stream Mach number and there is a minimum in shock strength at the design Mach number.

The effect of small changes in incidence at the design Mach number, again for aerofoil 1, is given in fig.16.

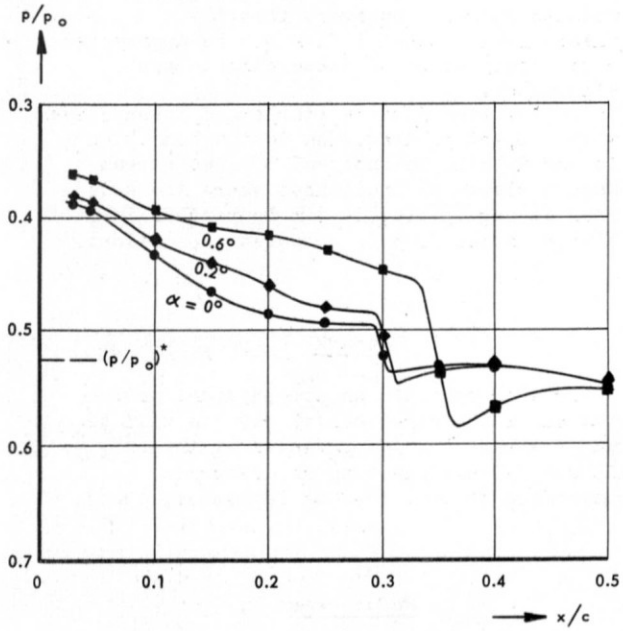

Figure 16 Effect of incidence on pressure distribution for aerofoil 1.

It appears that the shock wave, on the upper surface, grows in strength and moves downstream with increasing incidence.

The other aerofoils behave in much the same way as far as the effects of Mach number and incidence are concerned.

In order to see what these changes in shock strength mean, wake pressure measurements have been done to obtain drag coefficients. The dependence of drag coefficient on Mach number for different values of incidence for aerofoil 1 with free transition is given in fig.17.

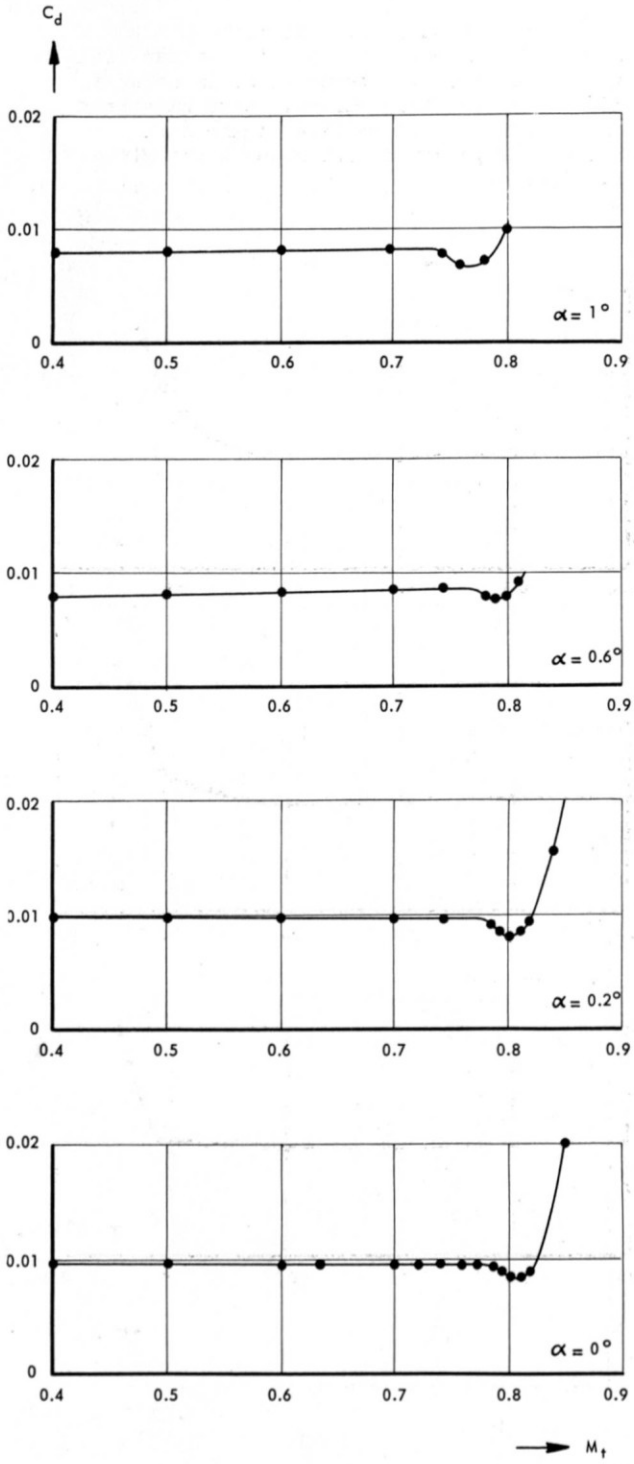

Figure 17 Drag coefficients for aerofoil 1; free transition.

It is shown that although there are always shock waves at off-design conditions, the wave drag remains negligibly small in a rather large interval.

Variations in transition point and separation effects make these drag values inconsistent. For instance, the further decrease in drag above the design Mach number

for $\alpha = 0$ is due to a rapid downstream movement of the transition point together with a disappearance of the separation. In order to obtain consistent drag values, tests have been made with fixed boundary layer transition upstream of separation. The results are given in fig.18.

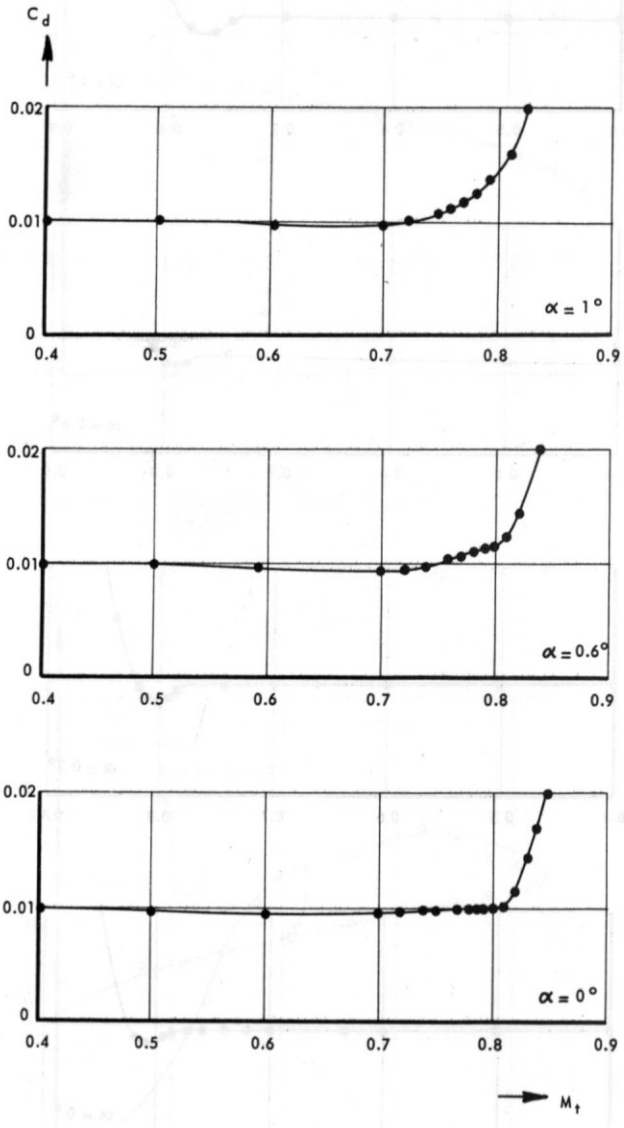

Figure 18 Drag coefficients for aerofoil 1; fixed transition.

It is shown that the dip in the drag curves has been filled up completely. It should be noted however, that due to the presence of the transition strip these is now a shock wave even at the design condition. It is to be expected that for full scale Reynolds numbers, and free transition, the shape of the drag curves will be somewhere between those of figs. 17 and 18.

Conclusions

The main results of the experiments are :

- the experimental data are in close agreement with the theoretical results and demonstrate clearly the physical relevance of the theoretical potential flows. At least in a practical sense, shock free flow has been found for all aerofoils.
- the differences between experiment and theory are due to modelimperfections and boundary layer effects. In particular laminar separations which are a consequence of the relatively low Reynolds number of the tests are reponsible for these differences. The results suggest, however, that the theoretical potential flow can be approached arbitrarily close if these effects are eliminated.
- the shock free flow is stable and insensitive with respect to drag. The design condition is embedded in an interval of free stream Mach numbers and incidences where the wave drag is negligible, it can be reached in a stable manner from neighbouring conditions.

Remark

Further comments on the physical interpretation of the experimental results will be given in a paper to be presented at the AGARD specialists' meeting on transonic aerodynamics (Paris, 18-20th September, 1968).

References

1. Nieuwland, G.Y., "Theoretical design of shock-free transonic flow around aerofoil sections". I.C.A.S. congress, London, 12-16 September, 1966. MacMillan 1967.

2. Nieuwland, G.Y., "Transonic potential flow around a family of quasi-elliptical aerofoil sections". N.L.R. Report TR.T.172 (1967).

3. Boerstoel, J.W., "A survey of symmetrical transonic potential flows around quasi-elliptical aerofoil sections". N.L.R. Report TR T.136 (1967).

4. Zwaaneveld, J., "Principal data of the N.L.L. pilot tunnel". N.L.R. Report MP.185 (1959).

5. Nieuwland, G.Y., Spee, B.M., "Transonic shock free flow,fact or fiction ?". Paper to be presented at the AGARD specialists' meeting on transonic flows. Paris, 18-20th September, 1968.